Journal of The Electrochemical Society, **162** (4) A704-A710 (2015)
0013-4651/2015/162(4)/A704/7/$33.00 © The Electrochemical Society

All Solid-State Lithium Batteries Assembled with Hybrid Solid Electrolytes

Yun-Chae Jung,[a] Sang-Min Lee,[b] Jeong-Hee Choi,[b] Seung Soon Jang,[c] and Dong-Won Kim[a,*,z]

[a]*Department of Chemical Engineering, Hanyang University, Seongdong-gu, Seoul 133-791, Korea*
[b]*Battery Research Center, Korea Electrotechnology Research Institute, Changwon-si, Gyeongsangnam-do 642-120, Korea*
[c]*School of Materials Science and Engineering, Georgia Institute of Technology, Atlanta, Georgia 30332-0245, USA*

The solvent-free hybrid solid electrolytes composed of lithium aluminum germanium phosphate (LAGP) and poly(ethylene oxide) (PEO) were prepared in the form of flexible film, and their electrochemical characteristics were investigated. The addition of ion-conductive LAGP powder into PEO-based solid polymer electrolyte improved the electrical and mechanical properties of solid electrolytes. For the hybrid solid electrolytes examined in this study, the optimum composition of LAGP was found to be about 60∼80 wt% in consideration of ionic conductivity, mechanical stability and formability for flexible thin film. The all solid-state Li/$LiFePO_4$ cell assembled with hybrid solid electrolyte delivered an initial discharge capacity of 137.6 mAh g^{-1} and exhibited good cycling stability at 55°C.

Manuscript submitted September 30, 2014; revised manuscript received January 14, 2015. Published February 5, 2015. This was Paper 675 presented at the Como, Italy, Meeting of the IMLB, June 10–14, 2014.

Lithium-ion batteries have rapidly become the dominant power sources for portable electronic devices, electric vehicles and energy storage systems, due to their high energy density and long cycle life.[1–3] However, safety issues still prevent full utilization of these batteries owing to the use of flammable liquid electrolytes, and thus safety problems have become a significant concern especially in large capacity applications such as electric vehicles and energy storage systems. In this respect, the development of all solid-state lithium batteries with non-flammable solid electrolytes may provide a fundamental solution to the safety issue of lithium batteries.[4–8] Inorganic solid electrolytes present potential advantages, such as absence of electrolyte leakage, high electrochemical stability, non-flammability, high thermal stability and absence of problems relating to vaporization of organic solvents. In the past decades, many studies have investigated NASICON-type solid ionic conductors with the general formula of $LiM_2(PO_4)_3$ (M = Ti, Ge, Sr, Zr, Sn, etc.). Among the NASICON-type lithium ion conductors reported so far, lithium aluminum germanium phosphate (LAGP, $Li_{1+x}Al_xGe_{2-x}(PO_4)_3$) has been of particular interest, because it exhibits superior stability in contact with lithium metal and has a relatively high ionic conductivity.[9–16] However, sheet manufacturing, especially using thin-film technologies for making large-scale batteries, is considered to be difficult because ceramic materials are hard and brittle. In addition, a lack of flexibility results in poor interfacial contact between inorganic solid electrolyte and electrodes in the cell during charge and discharge cycling. Therefore, the development of flexible solid-state electrolytes with improved interfacial contact has been one of the key issues for all solid-state lithium batteries. Solid polymer electrolytes based on poly(ethylene oxide) (PEO) present advantageous features such as flexibility in the shape of battery design, absence of leakage of organic solvents and better safety than liquid electrolytes.[1,17–21] However, they show poor ionic conductivity at ambient temperatures due to their tendency to crystallize and reduction of ionic mobility in the polymer electrolyte. Moreover, their poor mechanical properties at high temperature due to the melting transition may cause short circuits between two electrodes in cases where unusually high heat is generated. Hybrid solid electrolytes composed of inorganic solid electrolyte and flexible polymer electrolyte can synergistically combine the beneficial properties of both ceramics and polymers.[22–25] Inada et al. reported that processability and interfacial properties of solid electrolytes could be significantly improved by mixing glass ceramic electrolytes with flexible polymer materials.[22] However, they used insulating organic polymers such as styrene-butadiene copolymer or silicon rubber as binder, which may impede lithium ion conduction in the solid electrolyte. The electrochemical properties of composite electrolytes composed of lithium aluminum titanium phosphate and polyurethane, or lithium lanthanum titanium oxide and PEO have been investigated, but the cycling performance of the cells with composite electrolytes was not reported.[23,24] Inda et al. reported the electrochemical performance of solid-state lithium-ion cells with composite electrolytes based on $LiTi_2P_3O_{12}$ and poly(ethylene oxide-*co*-propylene oxide). The capacity retention of the cell was about 90% after 10 cycles at 60°C and low current rate (1/12C).[25]

In this study, the hybrid solid electrolytes composed of LAGP and PEO-based polymer electrolyte were prepared in the form of flexible thin film, and their electrochemical properties were investigated. PEO was used as an ion-conducting binder, because it is an ion-conductive polymer that transports lithium ions and it also has high flexibility owing to its low glass transition temperature. The effect of composition has been investigated to provide the hybrid solid electrolytes with high ionic conductivity and good mechanical properties. The hybrid solid electrolytes were applied to the all solid-state Li/$LiFePO_4$ cells, and their electrochemical performance was evaluated.

Experimental

Preparation of the hybrid solid electrolyte.— Stoichiometric amounts of lithium carbonate, aluminum oxide, germanium oxide and ammonium dihydrogen phosphate were used as the starting materials to prepare LAGP ($Li_{1.5}Al_{0.5}Ge_{1.5}(PO_4)_3$) by a conventional solid solution method. A small amount of B_2O_3 (0.05 wt% B_2O_3 to LAGP) was added in order to increase the ionic conductivity of LAGP, as previously reported.[26] The powder mixture was first thoroughly dispersed in isopropyl alcohol by ball milling for 24 h and dried at 25°C for 24 h to evaporate the volatile solvent. The powder mixture was heated to 700°C at a heating rate of 5°C min^{-1} in a tube furnace and held at that temperature for 2 h to release any volatile compounds. The powders were then reground followed by heating to 850°C with a heating rate of 5°C min^{-1} and calcinated at same temperature for 12 h in argon atmosphere. PEO (M_n = 200,000) and lithium perchlorate ($LiClO_4$) were purchased from Sigma-Aldrich, and the salt was used after vacuum drying at 100°C for 24 h. Hybrid solid electrolytes were prepared by a solution casting method, as schematically illustrated in Figure 1a. Appropriate amounts of PEO and $LiClO_4$ to give [EO]:[Li] ratio of 18:1 were dissolved in anhydrous acetonitrile, and the solution was stirred at 80°C for 12 h. A predetermined amount of LAGP powder was then added, and the solution was mixed using ballmilling for 24 h. The detailed compositions of LAGP, PEO and

*Electrochemical Society Active Member.
zE-mail: dongwonkim@hanyang.ac.kr

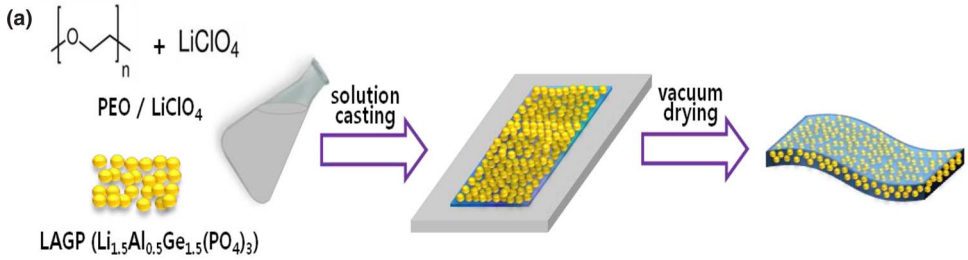

Figure 1. (a) Schematic presentation of preparation for hybrid solid electrolyte, and (b) photo image of hybrid solid electrolyte film (LAGP-70).

$LiClO_4$ in the hybrid solid electrolytes are given in Table I. When the complete homogenization of a mixture has occurred, the solution was cast on a flat Teflon plate using a doctor blade by allowing slow evaporation of solvent in an argon-filled glove box. Residual solvent was completely removed by heating the electrolyte film at 40°C under vacuum. The resulting hybrid solid electrolyte was in the form of freestanding flexible thin film, as shown in Figure 1b. The thickness of hybrid solid electrolytes ranged from 40 to 60 μm. In order to investigate the effect of ion-conductive LAGP in hybrid solid electrolytes, the inert Al_2O_3 particles (particle size: 2–4 nm, Aldrich) instead of LAGP were also used in preparing the composite polymer electrolytes. In order to prepare LAGP-based solid electrolyte in the form of pellet, LAGP powders were ground, pressed and sintered at 900°C for 12 h in an alumina crucible. The thickness of LAGP-based solid electrolyte was about 1000 μm.

Electrode preparation and cell assembly.— The $LiFePO_4$ active materials were kindly supplied by Hanwha Chemical. The composite positive electrode was prepared by coating an acetonitrile-based slurry containing $LiFePO_4$, PEO, $LiClO_4$ and Super P carbon (MMM Co.) (55 : 30.86 : 4.14 : 10 by weight) onto an Al foil. PEO was used as an ionic conductor as well as a polymer binder in the positive electrode. The electrode was dried under vacuum for 12 h at 40°C, and then roll pressed to enhance particulate contact and adhesion to the current collector. A geometrical area of the positive electrode was 1.54 cm^2, and the active mass loading in the positive electrode was about 3.6 mg cm^{-2}. The lithium negative electrode consisted of a 100-μm-thick lithium foil (Honjo Metal Co., Ltd.) that was pressed onto a copper current collector. All solid-state Li/$LiFePO_4$ cells were then assembled by sandwiching the hybrid solid electrolyte between the lithium negative electrode and the $LiFePO_4$ composite positive electrode, as schematically depicted in Figure 2. After the cell assembly process, the cells were kept at 55°C for 24 h in order to promote the interfacial contacts between hybrid solid electrolyte and $LiFePO_4$ composite positive electrode. All cells were assembled in a dry box filled with argon gas.

Table I. Composition of LAGP, PEO and $LiClO_4$ in the different solid electrolytes.

Electrolyte	LAGP (g)	PEO (g)	$LiClO_4$ (g)
PEO	0	2.0	0.268
LAGP-50	1.0	1.0	0.134
LAGP-60	1.2	0.8	0.107
LAGP-70	1.4	0.6	0.080
LAGP-80	1.6	0.4	0.054
LAGP-90	1.8	0.2	0.027
LAGP (sintered)	2.0	0	0

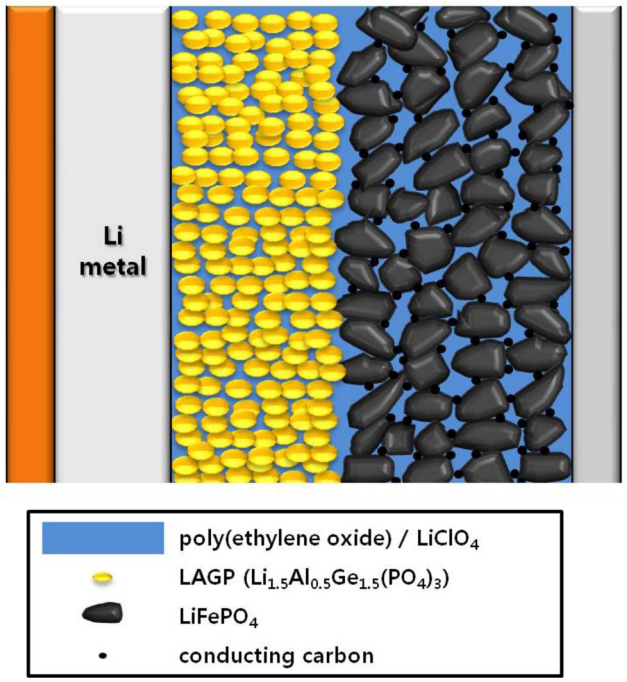

Figure 2. Schematic presentation of solid-state Li/$LiFePO_4$ cell assembled with hybrid solid electrolyte and composite positive electrode.

Characterization and measurements.— An cross section polisher (JEOL IB-09010CP) was used to prepare the cross-section of the hybrid solid electrolyte. Its cross-sectional morphology was examined using a scanning electron microscope (SEM, JEOL JSM-6300). The elemental distribution on the cross-sectional area of hybrid solid electrolyte was examined using energy dispersive X-ray spectroscopy (EDX). X-ray diffraction (XRD) patterns of LAGP, PEO and hybrid solid electrolytes were obtained using an X-ray diffractometer (Rigaku M2500) with Cu Kα radiation. For ionic conductivity measurements, the hybrid solid electrolyte was sandwiched between two disk-like stainless steel electrodes. AC impedance measurements were carried out using a Zahner Electrik IM6 impedance analyzer with amplitude of 10 mV. Each sample was allowed to equilibrate for 1 h at the required temperature before measurements. Linear sweep voltammetry (LSV) experiments were performed to investigate the electrochemical stability of the hybrid solid electrolytes on a platinum working electrode, with counter and reference electrodes of lithium metal, at a scanning rate of 1.0 mV s^{-1} and 55°C. Charge and discharge cycling tests of the solid-state Li/$LiFePO_4$ cells were conducted at a constant current rate over a voltage range of 2.6–4.0 V using battery testing equipment (WBCS 3000, Wonatech).

Results and Discussion

A FE-SEM image of the cross-sectional area for representative hybrid solid electrolyte (LAGP-70) is presented in Figure 3a. Although the LAGP powders exhibited heterogeneous particle size distribution

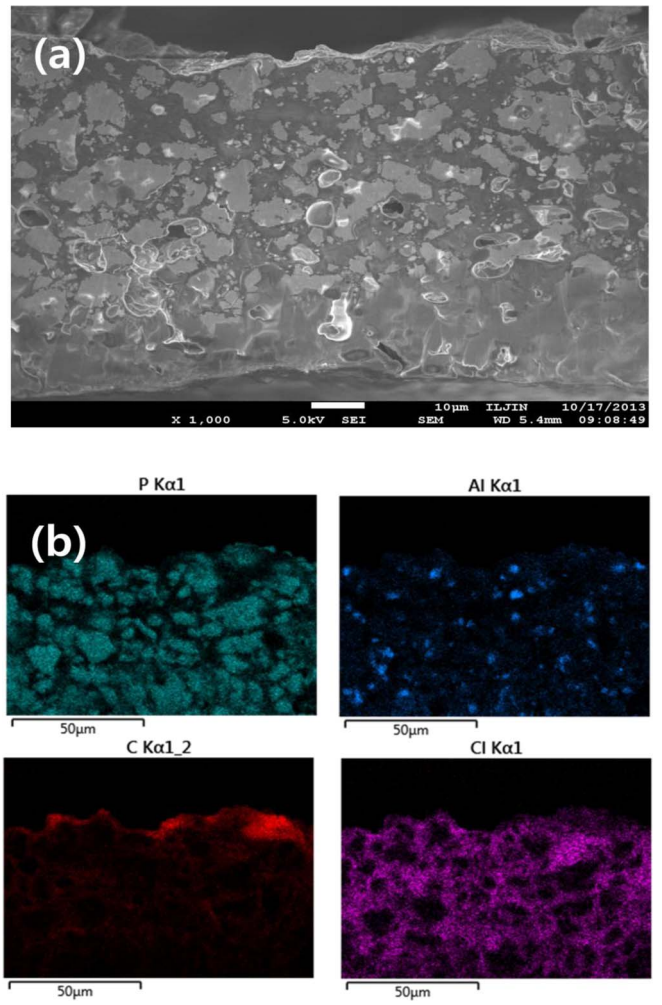

Figure 3. (a) Cross-sectional SEM image of hybrid solid electrolyte (LAGP-70), and (b) EDX mapping images of P, Al, C and Cl on the cross-section of LAGP-70.

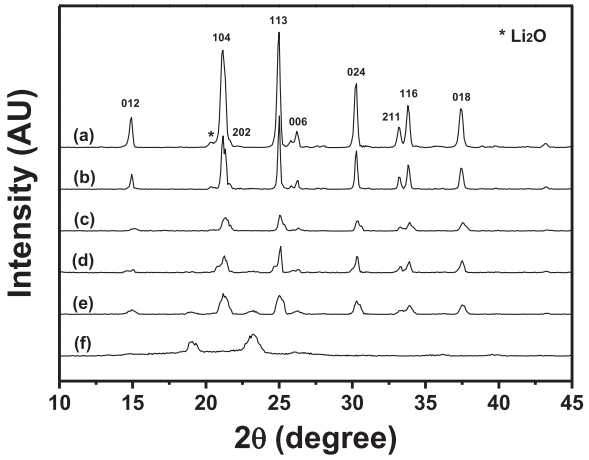

Figure 4. XRD patterns of (a) LAGP, (b) LAGP-90, (c) LAGP-80, (d) LAGP-70, (e) LAGP-60 and (f) PEO.

ranging from 0.2 to 15.0 μm, they were well embedded in solid polymer electrolyte composed of PEO and $LiClO_4$. Figure 3b shows the EDX mapping images of various elements (P, Al, C, Cl) on the cross-section of LAGP-70. It can be seen that P and Al elements arising from the LAGP particle are evenly distributed across the image. The chlorine atom from the $LiClO_4$ salt can be observed with carbon element in the PEO phase, suggesting that the salt is well dissolved in the PEO matrix.

Figure 4 shows the XRD patterns of LAGP, hybrid solid electrolytes and PEO. The XRD pattern obtained from LAGP powder corresponded to the LAGP phase with a minor impurity peak corresponding to Li_2O.[26] The hexagonal lattice parameters of the LAGP crystalline phase could be obtained using least squares fitting. The lattice parameters for the LAGP crystalline phase were determined to be $a = 8.284 \pm 0.001$ and $c = 20.541 \pm 0.046$ Å, respectively. These values are well matched with those reported in NASICON $LiGe_2(PO_4)_3$ crystalline phase ($a = 8.250$ Å and $c = 20.460$ Å).[10] The replacement of the Ge^{4+} (0.530 Å) by the larger Al^{3+} (0.535 Å) in the $LiGe_2(PO_4)_3$ crystalline phase resulted in structural modification that expands the lattice parameters.[9,10] The XRD pattern of PEO dissolving $LiClO_4$ exhibits two crystalline peaks at $2\theta = 19°$ and 23°, which are due to the ordering of polyether chains.[27,28] The intensity of crystalline peaks in PEO was significantly reduced by hybridizing PEO with LAGP. When the content of LAGP was higher than 70 wt%, the crystalline peaks completely disappeared, which can be attributed to the destruction effect of LAGP on the ordered arrangement of the polymer chains, thereby resulting in an increase of the amorphous phases in the hybrid solid electrolyte. The random distribution of LAGP particles with small size was enough to introduce the topological disorder to the solid polymer electrolyte. The reduction of crystalline phase in PEO by introducing the LAGP powder is expected to increase the ionic conductivity in the solid polymer electrolyte, as other ceramic fillers such as SiO_2, Al_2O_3 and TiO_2 enhance the ionic conduction in the composite polymer electrolytes.[29–31] As compared to pure LAGP, the crystalline peaks of LAGP in the hybrid solid electrolytes showed significant broadening due to the hybridization with less-crystalline organic polymer. By analyzing the XRD pattern of LAPG separated from hybrid solid electrolytes, it was confirmed that LAGP existed in the original form without any reaction/degradation in the hybrid film.

Nyquist plots of various hybrid solid electrolytes at 25°C are presented in Figure 5a. An equivalent circuit to describe the observed ac impedance spectra is shown in inset of Figure 5a, which represents a solid electrolyte sandwiched between two blocking electrodes. In this equivalent circuit, R_b is the bulk resistance of the solid electrolyte, CPE_b (constant phase element) denotes the bulk capacitance of the solid electrolyte, and CPE_{dl} corresponds to the double layer capacitance at the electrode/electrolyte interface.[32] Constant phase elements

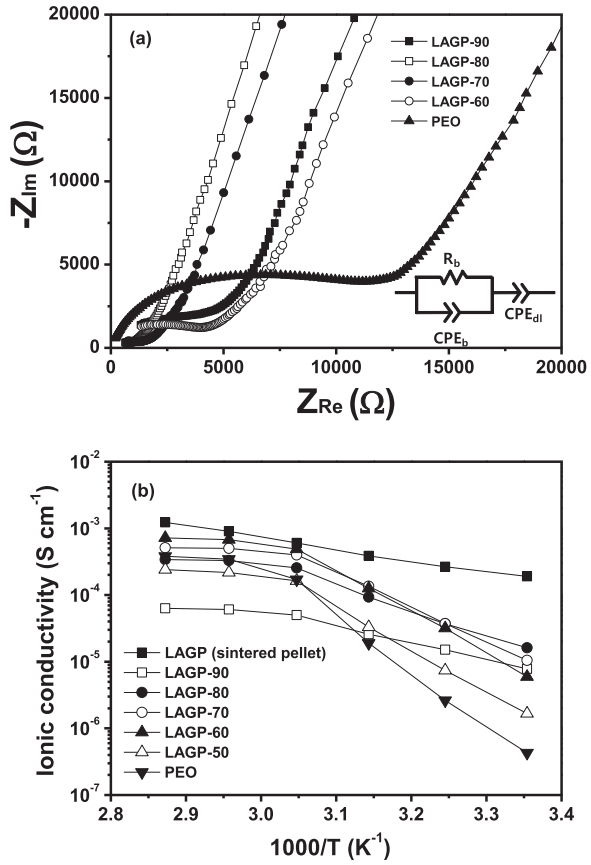

Figure 5. (a) AC impedance spectra of different solid electrolytes sandwiched between two blocking electrodes at 25°C, and (b) temperature dependence of ionic conductivity of various solid electrolytes with different compositions.

rather than capacitors were employed to describe non-idealities in ac impedance responses.[33] Ionic conductivities of the hybrid solid electrolyte were calculated using $\sigma = t / (R_b A)$, where t and A are is the thickness and area of the electrolyte film, respectively. The temperature dependence of ionic conductivities for hybrid solid electrolytes with different composition is shown in Figure 5b. The data presented here represent an average value of measurements with at least three different samples. The ionic conductivities of hybrid solid electrolytes were higher than those of solid polymer electrolytes prepared with PEO at temperatures lower than 45°C. This result suggests that the ion conduction in LAGP contributes to the ionic conductivity of hybrid solid electrolytes. It should be noted that the ionic conductivity of LAGP in the form of pellet is about 1.9×10^{-4} S cm^{-1} at room temperature, which is much higher than that of PEO-based solid polymer electrolyte (6.3×10^{-7} S cm^{-1}) at the same temperature. In order to investigate the contribution of ion-conductive LAGP powder to the ionic conductivity of hybrid solid electrolyte, we compared the ionic conductivities of hybrid solid electrolytes containing 70 wt% LAGP powder and 70 wt% Al_2O_3 particle, respectively. As a result, the hybrid solid electrolyte prepared with LAGP exhibited much higher ionic conductivity (1.0×10^{-5} S cm^{-1}) as compared to the composite polymer electrolyte containing Al_2O_3 particle (7.2×10^{-7} S cm^{-1}). Although the addition of inert Al_2O_3 particles can reduce the crystallinity of PEO-based solid polymer electrolyte, the particles may block the Li ion transport in the solid electrolyte containing high content of Al_2O_3 particles, since they are insulators by nature. Accordingly, the enhancement of ionic conductivity with an addition of LAGP is attributed to the incorporation of highly ionic conductive LAGP powder. The increase of ionic conductivity is also arising from the reduction in crystallinity of solid polymer electrolyte by adding the glass ceramic powders (LAGP). However, LAGP-90 containing high content of LAGP showed lower ionic conductivity due to the poor interfacial contacts between LAGP and PEO. In this hybrid electrolyte (LAGP-90), the content of PEO was too low for binding the glass ceramic powders efficiently. When LAGP content was lower than 60 wt%, the ionic conductivities were lower than those of hybrid solid electrolytes with higher LAGP content. The ionic conductivities of solid electrolyte prepared with LAPG (sintered LAGP pellet) were higher than those of hybrid solid electrolytes over the temperatures examined. However, it is noticeable that the solid electrolyte was not a flexible thin film but a rigid pellet with a thickness of 1000 μm. The PEO-based solid polymer electrolyte exhibited relatively high ionic conductivities at high temperatures; however, the dimensional stability was not good due to the melting of its crystalline phase at high temperature. From these results, LAGP-60, 70 and 80 are thought to be good hybrid solid electrolytes with regard to ionic conductivity, mechanical stability and formability for flexible film. They could be obtained as freestanding flexible films with a thickness of 45 μm, and their ionic conductivities were higher than 2.6×10^{-4} S cm^{-1} at 55°C.

The electrochemical stability of the hybrid solid electrolytes was evaluated by linear sweep voltammetric measurements at 55°C. LSV curves of the hybrid solid electrolytes and PEO-based polymer electrolyte are shown in Figure 6. In cathodic scan of PEO-based polymer electrolyte, a small reductive peak was observed around 1.43 V vs Li/Li$^+$, which may be associated with reductive decomposition of $LiClO_4$, as Abraham et al. previously reported.[34] All the electrolytes exhibited a large reductive current around 0 V vs Li/Li$^+$, which corresponded to the reductive deposition of lithium onto the electrode. With respect to anodic stability, the oxidative current started to

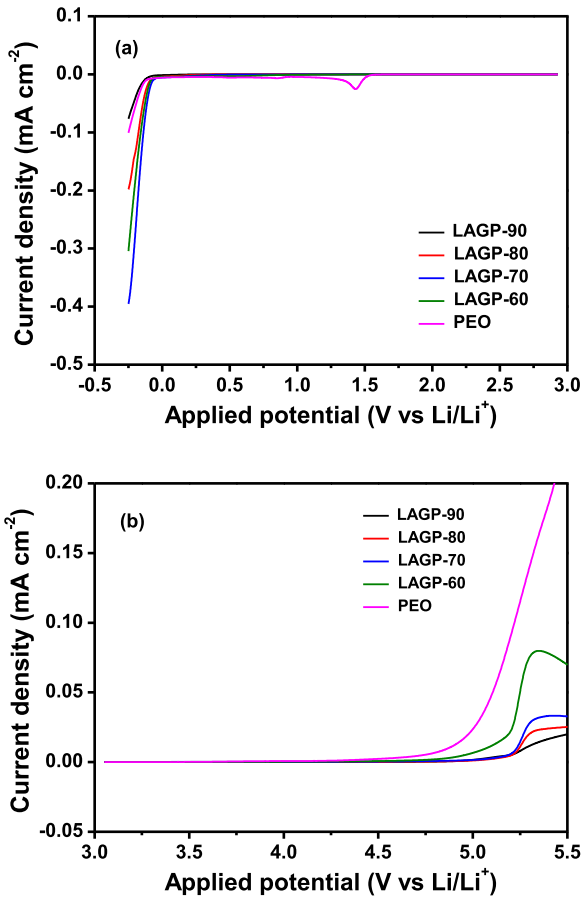

Figure 6. Linear sweep voltammograms of PEO-based solid polymer electrolyte and hybrid solid electrolytes at 55°C: (a) cathodic scan and (b) anodic scan (scan rate : 1 mV s^{-1}).

increase around 4.5 V vs. Li/Li^+ in the PEO-based polymer electrolyte, which can be attributed to the oxidative decomposition of PEO. On the other hand, the hybrid solid electrolytes exhibited oxidative stabilities higher than at least 4.75 V, indicating that hybridization of PEO with LAGP improves the electrochemical stability of the solid electrolyte. The anodic decomposition voltage was slightly increased with increasing the content of LAGP in the hybrid solid electrolyte. The enhanced anodic stabilities of hybrid solid electrolytes arise from the incorporation of LAGP that has an excellent oxidative stability at high potentials.[16] Based on these results, it is expected that the hybrid solid electrolytes composed of PEO and LAGP have wider electrochemical stability than PEO-based polymer electrolyte for electrochemical operation of the $Li/LiFePO_4$ cell.

We investigated the interfacial behavior of a lithium electrode in prolonged contact with hybrid solid electrolyte. Figure 7a shows the time evolution of the AC impedance spectra of Li/LAGP-70/Li cell under open-circuit potential conditions at 55°C. According to previous work, the depressed semicircle observed from medium to low frequency regions corresponds to formation of passivation film and charge transfer process.[35] Of particular our interest in these spectra is the total interfacial resistance, which is sum of the resistance of the passivation film and charge transfer resistance. Figure 7b presents the time evolution of interfacial resistance in the Li/solid electrolyte/Li cells assembled with different solid electrolytes. In PEO-based solid polymer electrolyte, the interfacial resistance continuously increased with time, which could be attributed to the gradual growth of a resistive surface layer due to the deleterious reaction of lithium electrode with thermodynamically unstable anions and impurities such as water in hygroscopic PEO-based polymer electrolyte. On the other hand, the interfacial resistances in the hybrid solid electrolytes were almost

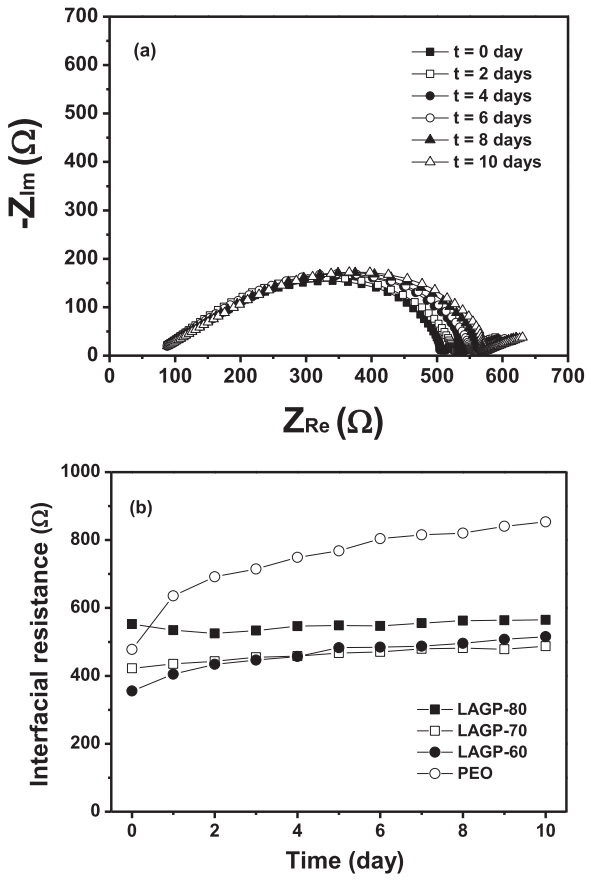

Figure 7. AC impedance spectra of a Li/LAGP-70/Li cell as a function of time at 55°C, and (b) the variation in interfacial resistance of the Li/solid electrolyte/Li cells as a function of time at 55°C.

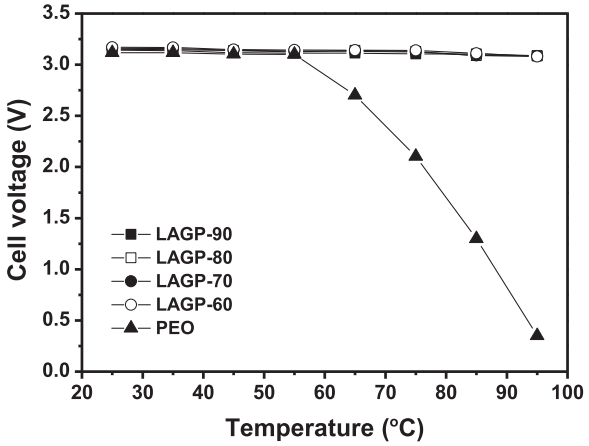

Figure 8. Open circuit voltages of the $Li/LiFePO_4$ cells assembled with different solid electrolytes, as a function of temperature.

constant, irrespective of time, which suggests no growth of the resistive surface film on the lithium electrode. As a result, the interfacial resistances in the cells with hybrid solid electrolyte were lower than one in the cell with PEO-based solid electrolyte after 10 days. It can be seen that the interfacial resistance was more stable in the hybrid solid electrolyte containing high content of LAGP. From these results, it is apparent that the addition of LAGP into PEO-based polymer electrolyte improved the interfacial stability. This result is consistent with previous works that the addition of ceramic powders such as Al_2O_3 and $LiAlO_2$ to the solid polymer electrolyte enhanced the interfacial stability.[29–31,35]

The solid-state $Li/LiFePO_4$ cells were assembled with different solid electrolytes. The $LiFePO_4$ was used as an active material in the positive electrode in our study due to its good cyclability, low cost, low toxicity and high thermal stability.[36–38] In order to evaluate the mechanical stability of various solid electrolytes, we measured open circuit voltages (OCV) of cells after storing the assembled cells at different temperatures for 1 h. Figure 8 shows the OCV of the cells assembled with different solid electrolytes, as a function of temperature. It is clearly seen that the cells with hybrid solid electrolytes maintain constant OCV over the temperatures investigated. In contrast, the cell with PEO-based solid polymer electrolyte exhibits a gradual drop in OCV with increasing temperature. The OCV drop can be ascribed to internal short-circuits of the cells due to the melting of crystalline PEO at high temperatures. The internal short-circuits of cell may eventually lead to fire or explosion of cells. These results demonstrate that the enhanced mechanical stability of hybrid solid electrolytes arising from the addition of LAGP powder allows fabrication of the safe solid-state $Li/LiFePO_4$ cells without any separator.

The solid-state $Li/LiFePO_4$ cells assembled with flexible hybrid solid electrolytes (LAGP-60, LAGP-70 and LAGP-80) with high ionic conductivity and good mechanical stability were subjected to charge and discharge cycles in the voltage range of 2.6–4.0 V at a constant current rate of 0.2C and 55°C. Figure 9a shows the charge-discharge curves of the 1st, 5th, 10th, 20th, 50th and 100th cycle of the $Li/LiFePO_4$ cell assembled with LAGP-70. The cell shows a potential plateau around 3.5 V, reflecting the common cycling behavior of the $LiFePO_4$ active material.[39] The cell delivered an initial discharge capacity of 137.6 mAh g^{-1} based on the active $LiFePO_4$ material in the positive electrode, with a coulombic efficiency of 96.5%. The irreversible capacity at the first cycle is mainly associated with the formation of solid electrolyte interphase (SEI) on the surface of lithium electrode as a result of reductive decomposition of electrolyte at the electrode, as previously reported.[40–42] Zaghib et al. reported that the reductive decomposition of the salt or traces of moisture in solid polymer electrolyte contributed to the initial irreversible capacity loss in solid-state lithium-ion polymer batteries.[40] According to other previous works on lithium polymer batteries, the SEI formed

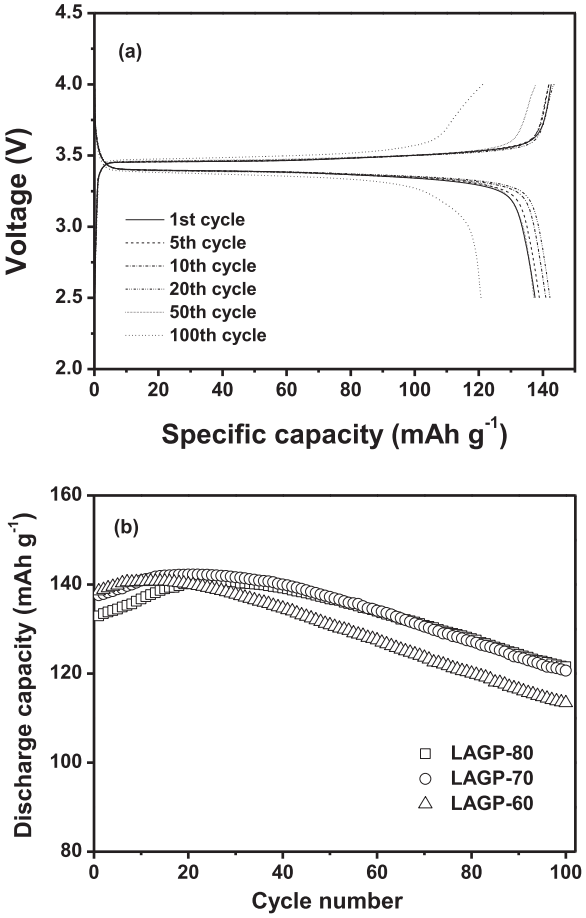

Figure 9. (a) Charge and discharge curves of the Li/LAGP-70/$LiFePO_4$ cell, and (b) discharge capacities of the Li/$LiFePO_4$ cells assembled with different hybrid solid electrolytes as the function of cycle number (0.2C, cutoff voltage: 2.6 – 4.0 V, 55°C).

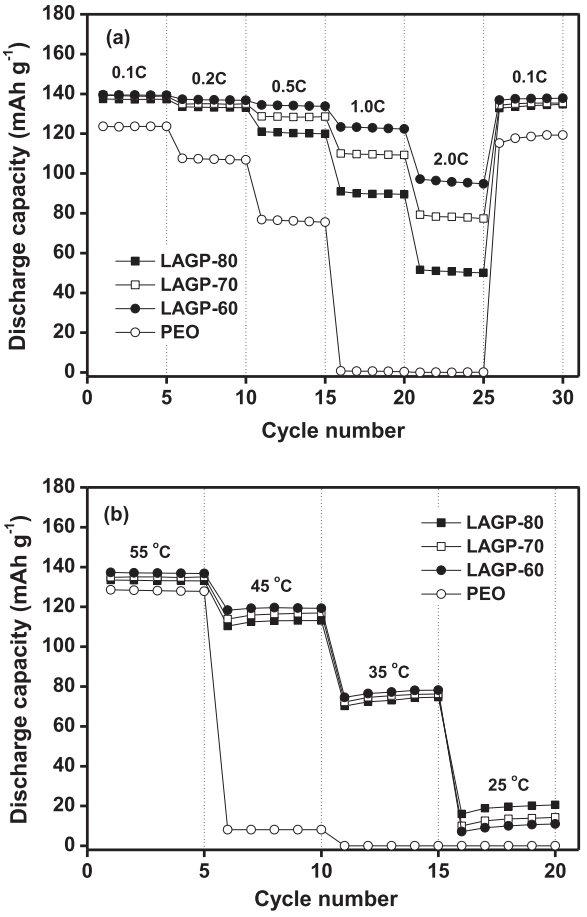

Figure 10. Discharge capacities of Li/$LiFePO_4$ cells assembled with different solid electrolytes as a function of (a) C rate and (b) temperature. Both C rate and temperature were changed after every 5 cycles.

on the lithium electrode mainly consisted of the salt decomposition products and the native film compounds such as Li_2CO_3, LiOH and Li_2O.[41,42] The coulombic efficiency of the Li/$LiFePO_4$ cell steadily increased and stabilized with the cycle number and was maintained at $>$ 99.0% throughout cycling after the initial few cycles. It is noticeable that the discharge capacity of the cell was gradually increased to the 20th cycle, and then slowly decreased with further cycling. The cell had a discharge capacity of 142.2 mAh g^{-1} at the 20th cycle. An initial increase in discharge capacity may be due to the fact that the ion transport in the hybrid solid electrolyte as well as the interfacial contacts between electrolyte and electrodes are improved during initial charge-discharge cycles of the cells. Figure 9b shows the discharge capacities of the Li/$LiFePO_4$ cells assembled with different hybrid solid electrolytes as a function of the cycle number. Discharge capacities of the cells decreased from their initial capacities of 133.0∼138.5 mAh g^{-1} to 113.4∼121.5 mAh g^{-1} at the 100th cycle, corresponding to 81.9∼91.3% of the initial values. The compact interfacial contacts between the flexible hybrid solid electrolyte and the composite $LiFePO_4$ positive electrode was contributed the good cycling stability. The capacity retention was improved with increasing the content of LAGP, which can be ascribed to the high electrochemical stability and good interfacial properties. Use of the electrochemically stable solid-state electrolyte (LAGP) may suppress harmful interfacial side reactions between the electrodes and the electrolyte, which results in good cycling stability.

Figure 10a shows the discharge capacities of the Li/$LiFePO_4$ cells assembled with different solid electrolytes, during experiments in which the C rate was increased every five cycles. The discharge capacities gradually decreased as the C rate was increased, thereby demonstrating polarization. Clearly, the discharge capacities of the cells employing hybrid solid electrolytes were higher than those of PEO-based cell for all C rates tested. Figure 10b compares the discharge capacities of the cells, which were obtained at different temperatures. The discharge capacities are found to be decreased with decreasing temperature, which are caused by both the high polarization due to the increase of the internal resistance of the cell and the reduced lithium ion diffusivity in the positive electrode. As expected in Figure 5b, the discharge capacities of the cells with hybrid solid electrolytes are much higher than those of cell with PEO-based solid electrolyte at lower temperatures. It should be noted that that cell with PEO-based solid electrolyte could not operate due to the high resistance of the solid electrolyte at temperatures lower than 35°C. In contrast, the cells assembled with hybrid solid electrolytes delivered discharge capacities ranging from 11.0 to 20.6 mAh g^{-1} at 25°C. This result is not sufficient as an ambient temperature performance, and must be improved further by increasing the ionic conductivities of hybrid solid electrolytes. More studies focusing flexible hybrid solid electrolytes with high ionic conductivity at ambient temperatures are currently in progress.

Conclusions

Hybrid solid electrolytes composed of LAGP and PEO were prepared in the form of flexible thin films, and their electrochemical properties were investigated. By hybridization of LAGP with PEO-based polymer electrolyte, both ionic conductivity and electrochemical stability could be enhanced. The Li/$LiFePO_4$ cells assembled with

hybrid solid electrolytes delivered high initial discharge capacities of 133.0∼138.5 mAh g^{-1} and exhibited good capacity retention at 55°C. The good cycling stability of the cells resulted from the high electrochemical stability of hybrid solid electrolyte and the good interfacial contacts with electrodes.

Acknowledgment

This research was supported by Korea Electrotechnology Research Institute (KERI) Primary Research Program through the Korea Research Council for Industrial Science & Technology (No. 13-12-N0101-23) and the Basic Science Research Program of the National Research Foundation of Korea (2014R1A2A2A01002154), funded by the Ministry of Science, ICT and Future Planning.

References

1. J. M. Tarascon and M. Armand, *Nature*, **414**, 359 (2001).
2. P. G. Bruce, B. Scrosati, and J. M. Tarascon, *Angew. Chem. Int. Ed.*, **47**, 2930 (2008).
3. V. Etacheri, R. Marom, R. Elazari, G. Salitra, and D. Aurbach, *Energy Environ. Sci.*, **4**, 3243 (2011).
4. P. Knauth, *Solid State Ionics*, **180**, 911 (2009).
5. J. W. Fergus, *J. Power Sources*, **195**, 4554 (2010).
6. E. Quartarone and P. Mustarelli, *Chem. Soc. Rev.*, **40**, 2525 (2011).
7. M. Nagao, H. Kitaura, A. Hayashi, and M. Tatsumisago, *J. Electrochem. Soc.*, **160**, A819 (2013).
8. L. Damen, J. Hassoun, M. Mastragostino, and B. Scrosati, *J. Power Sources*, **195**, 6902 (2010).
9. J. Fu, *Solid State Ionics*, **104**, 191 (1997).
10. B. V. R. Chowdari, G. V. Subba Rao, and G. Y. H. Lee, *Solid State Ionics*, **136–137**, 1067 (2000).
11. X. X. Xu, Z. Y. Wen, X. W. Wu, X. L. Yang, and Z. H. Gu, *J. Am. Ceram. Soc.*, **90**, 2802 (2007).
12. X. L. Yao, S. Xie, H. Q. Nian, and C. H. Chen, *J. Alloys Compd.*, **465**, 375 (2008).
13. J. S. Thokchom, N. Gupta, and B. Kumar, *J. Electrochem. Soc.*, **155**, A915 (2008).
14. J. S. Thokchom and B. Kumar, *J. Power Sources*, **185**, 480 (2008).
15. S. Rani, S. Sanghi, A. Agarwal, and N. Ahlawat, *J. Alloys Compd.*, **477**, 504 (2009).
16. J. K. Feng, L. Lu, and M. O. Lai, *J. Alloys Compd.*, **501**, 255 (2010).
17. M. B. Armand, *Solid State Ionics*, **69**, 309 (1994).
18. G. B. Appetecchi, D. Zane, and B. Scrosati, *J. Electrochem. Soc.*, **151**, A1369 (2004).
19. A. S. Arico, P. Bruce, B. Scrosati, J.-M. Tarascon, and W. Van Schalkwijk, *Nat. Mater.*, **4**, 366 (2005).
20. M. Armand and J.-M. Tarascon, *Nature*, **451**, 652 (2008).
21. E. Quartarone and P. Mustarelli, *Chem. Soc. Rev.*, **40**, 2525 (2011).
22. T. Inada, K. Takada, A. Kajiyama, M. Kouguchi, H. Sasaki, S. Kondo, M. Watanabe, M. Murayama, and R. Kanno, *Solid State Ionics*, **158**, 275 (2003).
23. K. M. Nairn, A. S. Best, P. J. Newman, D. R. MacFarlane, and M. Forsyth, *Solid State Ionics*, **121**, 115 (1999).
24. C. Wang, X.-W. Zhang, and A. J. Appleby, *J. Electrochem. Soc.*, **152**, A205 (2005).
25. Y. Inda, T. Katoh, and M. Baba, *J. of Power Sources*, **174**, 741 (2007).
26. H. S. Jadhav, M. S. Cho, R. S. Kalubarme, J. S. Lee, K. N. Jung, K. H. Shin, and C. J. Park, *J. of Power Sources*, **241**, 502 (2013).
27. S. A. Suthanthiraraj and D. J. Sheeba, *Ionics*, **13**, 447 (2007).
28. M. R. Johan, O. H. Shy, S. Ibrahim, S. M. Mohd Yassin, and T. Y. Hui, *Solid State Ionics*, **196**, 41 (2011).
29. J. E. Weston and B. C. J. Steele, *Solid State Ionics*, **7**, 75 (1982)
30. J. Fan and P. S. Fedkiw, *J. Electrochem. Soc.*, **144**, 399 (1997).
31. F. Croce, G. B. Appetecchi, L. Persi, and B. Scrosati, *Nature*, **394**, 456 (1998).
32. P. G. Bruce, in *Polymer Electrolyte Reviews*, J. R. McCallum and C. A. Vincent, Editors, Elsevier Applied Science, London (1987).
33. W. E. Tenhaeff, X. Yu, K. Hong, K. A. Perry, and N. J. Dudney, *J. Electrochem. Soc.*, **158**, A1143 (2011).
34. K. M. Abraham, M. Alamgir, and R. D. Moulton, *J. Electrochem. Soc.*, **138**, 921 (1991).
35. F. Croce and B. Scrosati, *J. Power Sources*, **43–44**, 9 (1993).
36. H. Joachin, T. D. Kaun, K. Zaghib, and J. Prakash, *J. Electrochem. Soc.*, **156**, A401 (2009).
37. L.-X. Yuan, Z.-H. Wang, W.-X. Zhang, X.-L. Hu, J.-T. Chen, Y.-H. Huang, and J. B. Goodenough, *Energy Environ. Sci.*, **4**, 269 (2011).
38. S. K. Martha, O. Haik, E. Zinigrad, I. Exnar, T. Drezen, J. H. Miners, and D. Aurbach, *J. Electrochem. Soc.*, **158**, A1115 (2011).
39. S. Yang, Y. Song, K. Ngala, P. Y. Zavalij, and M. S. Whittingham, *J. Power Sources*, **119–121**, 239 (2003).
40. K. Zaghib, M. Armand, and M. Gauthier, *J. Electrochem. Soc.*, **145**, 3135 (1998).
41. E. Peled, D. Golodnitsky, G. Ardel, and V. Eshkenazy, *Electrochim. Acta*, **40**, 2197 (1995).
42. C. Xu, B. Sun, T. Gustafsson, K. Edstrom, D. Brandell, and M. Hahlin, *J. Mater. Chem. A*, **2**, 7256 (2014).